Homenthalpic-flow approach for hypersonic inviscid non-equilibrium flows

Marie-Claude Ciccoli, Jean-Antoine Desideri

UNITÉ DE RECHERCHE
INRIA-SOPHIA ANTIPOLIS

Rapports de Recherche

N°1652

Programme 6
Calcul scientifique, Modélisation et Logiciel numérique

HOMENTHALPIC-FLOW APPROACH FOR HYPERSONIC INVISCID NON-EQUILIBRIUM FLOWS

Marie-Claude CICCOLI
Jean-Antoine DESIDERI

Avril 1992

Institut National
de Recherche
en Informatique
et en Automatique

Sophia Antipolis
B.P. 109
06561 Valbonne Cedex
France
Tél.: 93 65 77 77

HOMENTHALPIC-FLOW APPROACH FOR HYPERSONIC INVISCID NON-EQUILIBRIUM FLOWS

APPROCHE HOMENTHALPIQUE POUR LES ECOULEMENTS HYPERSONIQUES REACTIFS NON VISQUEUX

Marie-Claude CICCOLI
Jean-Antoine DESIDERI

I.N.R.I.A Sophia-Antipolis
2004, route des lucioles
06560 Valbonne

Contents

1 RESUME/ABSTRACT

On présente deux méthodes numériques pour la simulation d'écoulements hypersoniques réactifs non visqueux régis par les équations d'Euler couplées à un modèle chimique à 5 espèces et 17 réactions. On emploie des approximations spatiales décentrées de type Volumes Finis/Elements Finis.
On s'intéresse à l'efficacité des algorithmes en temps des deux méthodes. Les propriétés itératives de la méthode de base sont illustrées par les calculs d'écoulements autour de corps arrondis. En particulier, l'effet du nombre de Damkhöler (i.e. la taille de la géométrie) est mise en évidence.
On propose une variante à la méthode de base:
On sait que pour les écoulements externes avec conditions à l'infini uniformes, l'enthalpie totale est constante dans tout le domaine. Nous avons donc mis au point un algorithme qui conserve cette quantité et dans lequel l'équation différentielle de l'énergie est remplacée par son intégrale première (algébrique). Dans la section 4, on a adapté les décompositions de flux existantes à ce contexte et démontré leur validité. Enfin, on présente une expérimentation numérique de ce nouvel algorithme au premier et au second ordre en espace.

Two different methods for the numerical simulation of steady, inviscid, non-equilibrium reactive flow governed by Euler equations augmented by a 5-species 17-reaction finite-rate dissociation model are studied. The employed approximations are based on a conservative mixed Finite-Volume/Finite-Element upwind formulation.
The study concentrates on the efficiency of the pseudo-time integration methods as iterative algorithms. The iterative properties of the basic method are demonstrated by various computations of flow fields around blunt bodies. In particular, the effect of varying the global Damkhöler number (i.e. the size of the geometry) is illustrated.
A variant of the basic method is proposed:
We know that for steady (external) flows with uniform free-stream, the total enthalpy is constant throughout the domain. Hence, an algorithm which conserves this quantity has been implemented in which the energy equation (in differential form) is not solved but replaced by its (algebraic) first integral. The extension of existing flux-vector splittings (FVS) to this context where one less PDE is solved and one algebraic constraint is enforced, is examined in Section 4 in which the FVS is demonstrated to be proper. Finally, the efficiency of the proposed new approach is assessed by numerical experiments for first and second order approximation schemes.

2 MATHEMATICAL MODEL

2.1 GOVERNING EQUATIONS

An inviscid non-equilibrium reactive flow is modeled by the Euler equations and a set of species conservation equations :

$$W_t + F_1(W)_x + F_2(W)_y = 0 \tag{1}$$

$$(\rho_s)_t + div(\rho_s \vec{V}) = \Omega_s \tag{2}$$

with :

$$W = \begin{pmatrix} \rho \\ \rho u \\ \rho v \\ E \end{pmatrix} \quad F_1(W) = \begin{pmatrix} \rho u \\ \rho u^2 + p \\ \rho uv \\ u(E+p) \end{pmatrix} \quad F_2(W) = \begin{pmatrix} \rho v \\ \rho uv \\ \rho v^2 + p \\ v(E+p) \end{pmatrix}$$

where : ρ is the density
u, v are the velocity components
p is the pressure
E is the total energy
N is the number of species
ρ_s = is the partial density of the species s
$= \rho\ Y_s$ (Y_s = mass fraction)
Ω_s is the production rate of the species s

Each species is a perfect gas and the pressure is given by:

$$p = \rho \mathcal{R} T \sum_{s=1}^{N} \frac{Y_s}{m_s}$$

where : $\mathcal{R}$ is the perfect gas universal constant
T is the temperature
m_s is the molar mass of the species s.

Moreover, the energy must be expressed in terms of the temperature and the composition. We assume thermal equilibrium (only one temperature), and :

$$E = E_c + H_0 + E_{c_v} + E_{vib}$$

where : $E_c = \frac{1}{2}\,\rho\,(u^2+v^2)$ is the kinetic energy

$H_0 = \sum_{s=1}^{P} \rho Y_s h_s^0$ is the energy of formation

$E_{c_v} = \sum_{s=1}^{N} \rho Y_s C_{v_s} T$ is the internal energy

$E_{vib} = \sum_{s=P}^{N} \rho Y_s \frac{\mathcal{R}_s \Theta_{v_s}}{\exp \frac{\Theta_{v_s}}{T} - 1}$ is the vibrational energy

h_s^0 is the enthalpy of formation of the species s

$\mathcal{R}_s = \frac{\mathcal{R}}{m_S}$

the indices $s = P, ..., N$ are related to the species whose vibrational state is supposed to be at equilibrium at temperature T.

In the species convection equations (2), the source term, Ω_s, is the production rate of species s. Its exact expression is detailed by the model that is described in the next subsection.

2.2 CHEMICAL MODEL

The fluid we consider is air which, in normal temperature conditions is principally composed of molecular oxygen and nitrogen. The temperature range of typical hypersonic flows is such that dissociation effects are important. At the front of a reentry body, in the shock, the temperature may reach very high values (about 25000 K). As a result, O_2 and N_2 dissociate into the following species : N_2, O_2, NO, N, O, NO^+, O^+, N^+, O^-, N^-,... . Our model assumes no ionization. The following five species are considered : O, N, NO, O_2, N_2. We employ the following 17-reaction scheme :

$$\begin{array}{rcll} O_2 + X & \rightleftharpoons & O + O + X & \\ N_2 + X & \rightleftharpoons & N + N + X & \\ NO + X & \rightleftharpoons & N + O + X & \text{Zel'dovich} \\ NO + O & \rightleftharpoons & O_2 + N & \text{model [1]} \\ N_2 + O & \rightleftharpoons & NO + N & \end{array}$$

where X stands for an arbitrary species. The species formation reactions from N_2 and O_2 are endothermic; the effect of these dissociations is thus to reduce the temperature importantly.

The definition of the mass fractions gives :

$$\sum_{s=1}^{5} Y_s = 1 \tag{3}$$

The fluid is inviscid and species diffusion is neglected, and since the freestream conditions are constant, the atoms of N and O are globally conserved. This gives :

$$\frac{\frac{Y_{N_2}}{m_n} + \frac{Y_N}{m_N} + \frac{Y_{NO}}{m_{no}}}{\frac{Y_{O_2}}{m_O} + \frac{Y_O}{m_O} + \frac{Y_{NO}}{m_{NO}}} = \frac{79}{21} \tag{4}$$

because in the freestream, air is composed of 79% of nutrogen and 21% of oxygen.
Combining (3) and (4) yields :

$$\begin{cases} Y_{O_2} = \dfrac{24}{103} - Y_O - \dfrac{8}{15} Y_{NO} \\ \\ Y_{N_2} = \dfrac{79}{103} - Y_N - \dfrac{7}{15} Y_{NO} \end{cases}$$

This permits us to solve only three conservation species equations :

$$(\rho Y_s)_t + div(\rho Y_s \vec{V}) = \Omega_s \quad s = 1, ..., 3$$

The expression of the production rate Ω is given by the Park model [2].

3 BASIC NUMERICAL APPROXIMATION

We are interested in steady solutions. We obtain them by time integration. An existing code capable of solving the Euler equations over arbitrary unstructured meshes has been adapted to the case of a reactive flow. The method we have adopted to solve the Euler and species equations consists in fractioning the time step into two substeps : first the Euler equations are advanced of Δt keeping the composition frozen but not uniform, second the species convection equations are advanced of Δt keeping the usual conservative variables $\rho, \rho u, \rho v, E$ constant. The two substeps are realized implicitly [5]. Such approach is sometimes referred to by other authors as a "weakly-coupled" approach. However, in [5], we observed that when the energy equation is solved between the two substeps and thus an updated value of the temperature is employed in the chemistry substep, the coupling was significantly enhanced to make this approach in certain cases significantly more efficient than strongly coupled algorithms (see section 3.3).

3.1 SOLUTION OF THE EULER EQUATIONS

3.1.1 INERT GAS

To simplify the presentation, we consider here the conservative Euler equations in the 1-D case :

$$W_t + F(W)_x = 0$$

The 2 D case is presented in 3.4.
We suppose that the variables are piecewise constant :

$$W^n(x) = W_i^n \qquad for \quad x \in]x_{i-\frac{1}{2}}, x_{i+\frac{1}{2}}[$$

$$\begin{array}{rll} where: & W^n(x) = W(x,t^n) & with \quad t^n = n \triangle t \\ & W_i^n = W(x_i,t^n) & with \quad x_i = i \triangle x \end{array}$$

By integrating (1) over $]x_{i-\frac{1}{2}}, x_{i+\frac{1}{2}}[$, we obtain the following explicit conservative scheme :

$$\frac{W_i^{n+1} - W_i^n}{\triangle t} + \frac{F_{i+\frac{1}{2}} - F_{i-\frac{1}{2}}}{\triangle x} = 0 \qquad (5)$$

The numerical fluxes $F_{i+\frac{1}{2}}^n$ are evaluated by means of a numerical function

noted Φ :

$$F_{i+\frac{1}{2}} = \Phi(W_i, W_{i+1})$$

We suppose that Φ is consistent : $\Phi(U,U) = F(U)$.
We use the Van Leer flux-vector splitting [3] :

$$\Phi^{VL}(U,V) = \mathcal{F}^+(U) + \mathcal{F}^-(V)$$

where : $\mathcal{F}^+(\mathrm{U}) + \mathcal{F}^-(\mathrm{U}) = \mathrm{F(U)}$ (consistency)
We note $f_1^+ = \frac{1}{4}\rho\, c \left(\frac{u}{c}+1\right)^2$ (the "plus part" of the mass flux), the flux $\mathcal{F}^+$ is given by

$$\mathcal{F}^+ = \begin{cases} F & \text{if } u \geq c \ , \\ \begin{pmatrix} f_1^+ \\ \frac{f_1^+}{\gamma}((\gamma-1)u+2c) \\ \frac{f_1^+}{2(\gamma^2-1)}((\gamma-1)u+2c)^2 \end{pmatrix} & \text{if } -c < u < c \ , \\ 0 & \text{if } u \leq -c \ , \end{cases}$$

and $\mathcal{F}^-$ is obtained by :

$$\mathcal{F}^- = F - \mathcal{F}^+ \qquad (consistency).$$

We calculate the fluxes Φ^{VL} at the time step n+1.
We linearize $\Phi^{VL^{n+1}}$:

$$\Phi^{VL^{n+1}}_{i+\frac{1}{2}} = \Phi^{VL^n}_{i+\frac{1}{2}} + \mathcal{F}_i^{n+'}(W_i^{n+1} - W_i^n) + \mathcal{F}_{i+1}^{n-'}(W_{i+1}^{n+1} - W_{i+1}^n)$$

We note :

$$\delta W^{n+1} = W^{n+1} - W^n$$

So, we obtain the following "Delta formulation" of the discrete equation at node i :

$$\boxed{\left(\frac{\triangle x}{\triangle t} Id + \mathcal{F}_i^{n+'} - \mathcal{F}_i^{n-'}\right)\delta W_i^{n+1} + \mathcal{F}_{i+1}^{n-'}\delta W_{i+1}^{n+1} - \mathcal{F}_{i-1}^{n+'}\delta W_{i-1}^{n+1} = -\Phi^{VL^n}_{i+\frac{1}{2}} + \Phi^{VL^n}_{i-\frac{1}{2}}} \tag{6}$$

This scheme requires at each time step the solution of a linear system of dimension (4 × NS)×(4 × NS) where NS is the number of points in the mesh. This solution is made by the Gauss-Seidel iteration carried to partial convergence.

3.1.2 REACTIVE GAS

In the case of a perfect gas, we have :

$$\mathrm{p} = (\ \gamma - 1\ )\ \rho\ \varepsilon$$

where : $\gamma = \dfrac{C_p}{C_v}$

ε : is the internal energy

$\varepsilon = E - E_c = H_0 + E_{C_v} + E_{vib}$

(cf. 2.1 for the expressions of $H_0, E_{C_v} et E_{vib}$).

Then, we have : $$c^2 = \frac{\gamma p}{\rho}$$

In the general case of a reacting gas, $p = p(\rho, \varepsilon)$. We define a parameter $\tilde{\gamma}$ called "pseudo-γ" or "γ-équivalent" [4] which is such that :

$$p = (\tilde{\gamma} - 1)\rho\varepsilon$$

Afterwards, the "$pseudo - \gamma$" $\tilde{\gamma}$ is simply written γ. We deduce a pseudo-speed of sound c and a pseudo Mach number M such that :

$$c^2 = \frac{\gamma p}{\rho}\ \ et\ \ M = \frac{V}{c}$$

These variables are injected in the usual expressions of the Van Leer flux vector splitting. Examples of usage of this approximation scheme are given by [4] [7].

3.2 SOLUTION OF THE SPECIES EQUATIONS

When we solve the species equations at the time step t_{n+1}, the other variable $(\rho, \rho u, \rho v, E)$ are taken at the time step t_{n+1}. The following implicit scheme and its performances are studied in [5].

The implicit scheme of (2) writes :

$$\frac{(\rho Y)_i^{n+1} - (\rho Y)_i^n}{\triangle t} + \frac{(\rho Y \vec{V})_{i+\frac{1}{2}}^{n+1} - (\rho Y \vec{V})_{i-\frac{1}{2}}^{n+1}}{\triangle x} = \Omega_i^n + \Omega_i^{n'} \delta(\rho Y)_i^{n+1}$$

To calculate $(\rho Y \vec{V})_{i+\frac{1}{2}}$, we use a numerical flux function Ψ :

$$(\rho Y \vec{V})_{i+\frac{1}{2}} = \Psi_{i+\frac{1}{2}} = \Psi((\rho Y)_i, (\rho Y)_{i+1})$$

where [6] :

$$\Psi((\rho Y)_i, (\rho Y)_{i+1}) = Y_i \mathcal{F}_{1i}^+ + Y_{i+1} \mathcal{F}_{1i+1}^-$$

where : $\mathcal{F}_1^+$ et $\mathcal{F}_1^-$ are the first components of $\mathcal{F}^+$ et $\mathcal{F}^-$.

The numerical fluxes $\Psi_{i+\frac{1}{2}}^{n+1}$ are written :

$$\Psi_{i+\frac{1}{2}}^{n+1} = Y_i^{n+1} \mathcal{F}_{1i}^{n+1+} + Y_{i+1}^{n+1} \mathcal{F}_{1i+1}^{n+1-}$$

We linearize $\Psi_{i+\frac{1}{2}}^{n+1}$:

$$\Psi_{i+\frac{1}{2}}^{n+1} = \Psi_{i+\frac{1}{2}}^n + \frac{\partial \Psi_{i+\frac{1}{2}}^n}{\partial (\rho Y)_i^n} \delta(\rho Y)_i^{n+1} + \frac{\partial \Psi_{i+\frac{1}{2}}^n}{\partial (\rho Y)_{i+1}^n} \delta(\rho Y)_{i+1}^{n+1}$$

Now, we have : $\dfrac{\partial \Psi_{i+\frac{1}{2}}^n}{\partial (\rho Y)_i^n}$ et $\dfrac{\partial \Psi_{i+\frac{1}{2}}^n}{\partial (\rho Y)_{i+1}^n}$:

$$\Psi_{i+\frac{1}{2}}^n = Y_i^n \mathcal{F}_{1i}^{n+} + Y_{i+1}^n \mathcal{F}_{1i+1}^{n-}$$

which can be written :

$$\Psi_{i+\frac{1}{2}}^n = (\rho Y)_i^n \frac{\mathcal{F}_{1i}^{n+}}{\rho_i^n} + (\rho Y)_{i+1}^n \frac{\mathcal{F}_{1i+1}^{n-}}{\rho_{i+1}^n}$$

The numerical fluxes $\mathcal{F}^+$ et $\mathcal{F}^-$ are homogenous of degree one in ρ :

$$\frac{\partial \Psi_{i+\frac{1}{2}}^n}{\partial (\rho Y)_i^n} = \frac{\mathcal{F}_{1i}^{n+}}{\rho_i^n} \quad and \quad \frac{\partial \Psi_{i+\frac{1}{2}}^n}{\partial (\rho Y)_{i+1}^n} = \frac{\mathcal{F}_{1i+1}^{n-}}{\rho_{i+1}^n}$$

The scheme applied to the chemistry equations becomes :

$$\boxed{\begin{array}{c}\left(\frac{\triangle x}{\triangle t}Id - \triangle x\Omega_i'^n + \frac{\mathcal{F}_{1,i}^{n+}}{\rho_i^n} - \frac{\mathcal{F}_{1,i}^{n-}}{\rho_i^n}\right)\delta(\rho Y)_i^{n+1} \\ + \frac{\mathcal{F}_{1,i+1}^{n,-}}{\rho_{i+1}^n}\delta(\rho Y)_{i+1}^{n+1} - \frac{\mathcal{F}_{1,i-1}^{n,+}}{\rho_{i-1}^n}\delta(\rho Y)_{i-1}^{n+1} \\ = \triangle x\Omega_i^n - \Psi_{i+\frac{1}{2}}^n + \Psi_{i-\frac{1}{2}}^n\end{array}} \quad (7)$$

This scheme requires at each time step the solution of a linear system of dimension (3 $\times$ NS)$\times$(3 $\times$ NS) where NS is the number of points in the mesh. This solution is made by the Gauss-Seidel iteration carried to partial convergence.

3.3 TEMPERATURE CALCULATION

The fluid is taken at thermal equilibrium, hence only one temperature T is introduced.
The calculation of this temperature is made from the following expression of the energy :

$$E = E_c + H_0 + E_{c_v} + E_{vib}$$

When we neglect the vibrational energy E_{vib}, E is a linear function of the temperature. But in the general case ($E_{vib} \neq 0$), we must iterate.
We initialize the temperature at the time step t^{n+1} by the value T^n at the time step t^n ($T^{(0)} = T^n$), and then we calculate the temperature from the state law and we update the energy to evaluate the pressure and the γ :

$$\begin{aligned} T^{(\alpha+1)} &= \frac{p}{\rho R} \\ E &= E_c + H_0 + E_{cv}(T^{(\alpha+1)}) + E_{vib}(T^{(\alpha+1)}) \end{aligned}$$

To make the coupling between the species and the temperature stronger and to increase the robustness of the implicit scheme, we update the temperature between the Euler step and the chemistry step.

A global time iteration can be summerized by the following chart :

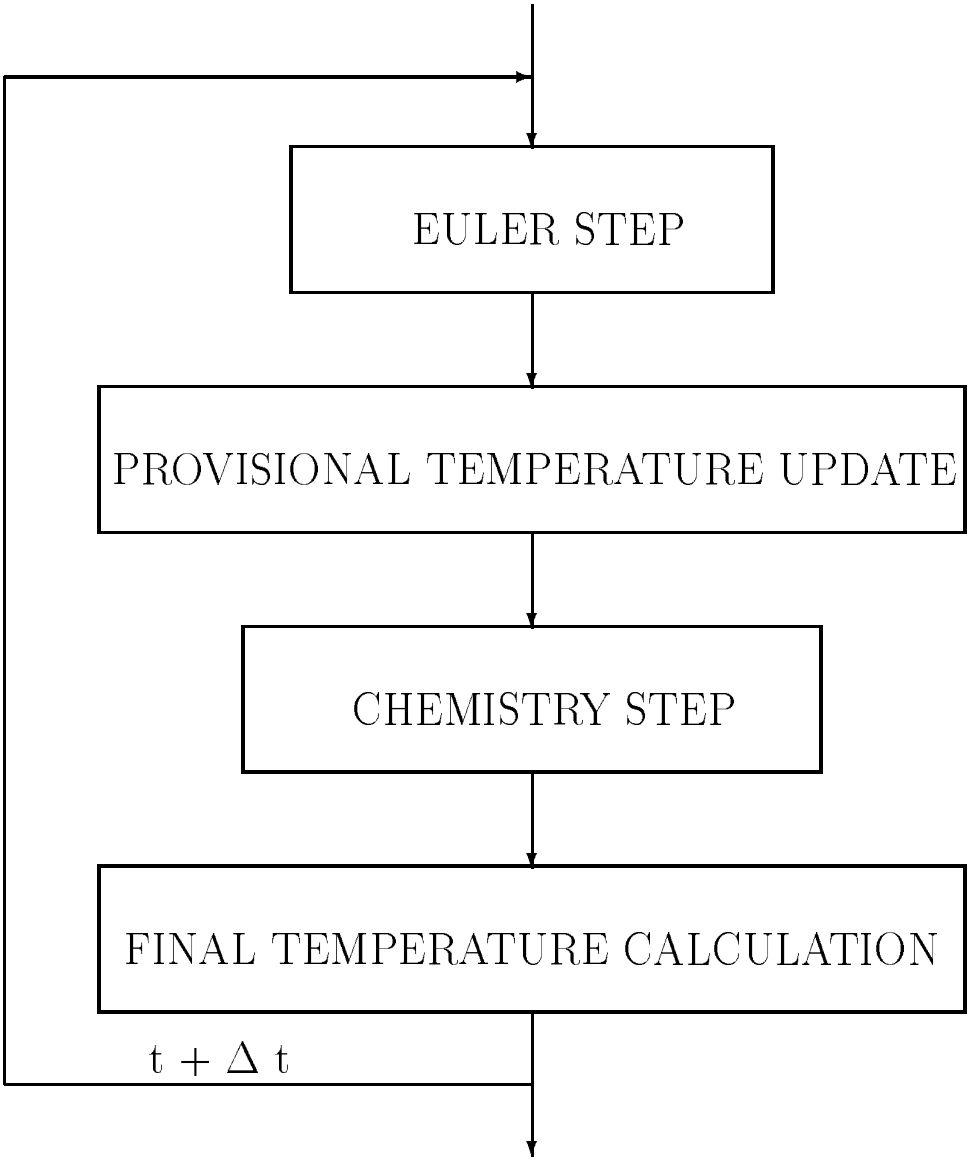
EULER STEP
PROVISIONAL TEMPERATURE UPDATE
CHEMISTRY STEP
FINAL TEMPERATURE CALCULATION
t + Δ t

3.4 2.D EXTENSION

To be complete, we briefly present in this section how two-dimensional implementations are carried. In the 2-D case, the approximations are obtained as extensions of the 1-D case.
The spatial approximation uses a finite volume/finite element formulations. We construct the cell C_i around the node i with the gravity centers of the triangles whose i is a node. We note ∂C_i the boundary of C_i, A_i the area and $\vec{\nu} = (\nu_1, \nu_2)$ the normal vector to it.

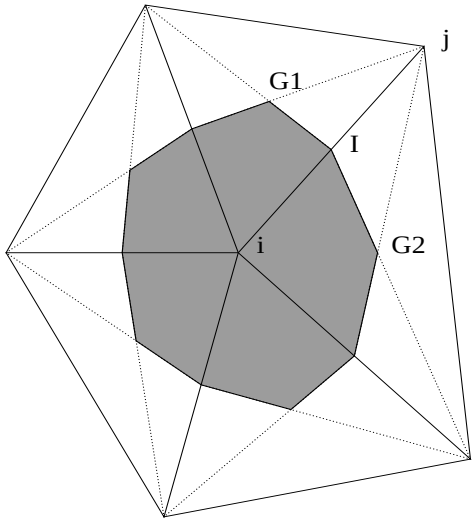

Cell of integration C_i

After applying Green's formula, a weak formulation of (1) writes :

$$\int_{C_i} W_t + \int_{\partial C_i} (\nu_1 F_1 + \nu_2 F_2) d\sigma = 0$$

A first-order finite-volume approximation of the above equation is given by :

$$A_i \frac{W_i^{n+1} - W_i^n}{\triangle t} + \int_{\partial C_i} (\nu_1 F_1^n + \nu_2 F_2^n) d\sigma = 0 \tag{8}$$

This equation can also be written in the form :

$$A_i \frac{W_i^{n+1} - W_i^n}{\triangle t} + \sum_{j \ voisin \ de \ i} \int_{\partial C_i \cap \partial C_j} (\nu_{1ij} F_1^n + \nu_{2ij} F_2^n) d\sigma = 0 \tag{9}$$

We note :

$$\vec{\eta}_{ij} = \int_{\partial C_i \cap \partial C_j} \vec{\nu}_{ij} d\sigma$$

The Van Leer flux is :

$$\Phi^{VL}(W_i, W_j, \vec{\eta}_{ij}) = \eta_{1ij}(\mathcal{F}_i^{1+} + \mathcal{F}_j^{1-}) + \eta_{2ij}(\mathcal{F}_i^{2+} + \mathcal{F}_j^{2-})$$

The chemistry numerical flux Ψ becomes :

$$\Psi((\rho Y)_i, (\rho Y)_j, \vec{\eta}_{ij}) = \eta_{1ij}(Y_i \mathcal{F}_{1i}^{1+} + Y_j \mathcal{F}_{1j}^{1-}) + \eta_{2ij}(Y_i \mathcal{F}_{1i}^{2+} + Y_j \mathcal{F}_{1j}^{2-})$$

$$\boxed{\Psi((\rho Y)_i, (\rho Y)_j, \vec{\eta}_{ij}) = Y_i \left[\eta_{1ij}\mathcal{F}_{1i}^{1+} + \eta_{2ij}\mathcal{F}_{1i}^{2+}\right] + Y_j \left[\eta_{1ij}\mathcal{F}_{1j}^{1-} + \eta_{2ij}\mathcal{F}_{1j}^{2-}\right]}$$

4 HOMENTHALPIC-FLOW APPROACH

4.1 PRESENTATION

At steady-state, the energy equation for inviscid flow writes :

$$div(\vec{V}(E+p)) = 0$$

but, we can write : $div(\rho\vec{V}(\frac{E+p}{\rho}) = div(\rho\vec{V})\frac{E+p}{\rho} + \rho\vec{V}.\bigtriangledown\frac{E+p}{\rho}$

The steady solution also verifies : $div(\rho\vec{V}) = 0$, hence :

$$\vec{V}.\bigtriangledown\frac{E+p}{\rho} = 0$$

This means that $h = \frac{E+p}{\rho}$ (total enthalpy per unit mass) is constant on each streamline.

If at infinity, the flow is uniform, the quantity h is constant throughout the entire domain. This is true also through shocks by virtue of the jump condition: $h_1 = h_2$. Such flow is said to be "homenthalpic". In such case, one can avoid solving the energy equation in differential form, but instead employ its first integral ($h = h_\infty$) as an algebraic constraint allowing us to calculate E in the following way :

$$\boxed{E = \rho h_\infty - p}$$

where h_∞ is the given freestream enthalpy.

So, for the Euler substep, we solve only the three differential equations governing $\rho, \rho u, \rho v$. In such an approach, we need to calculate the new jacobians of the fluxes. This calculation is described in the following paragraph.

4.2 JACOBIAN CALCULATIONS

According to the presentation of the basic method, we present here the 1-D calculations, the 2-D fluxes are evaluated, like for the basic ones, as their extensions.

4.2.1 Jacobians of the Van Leer fluxes

For the Eulerian part of the equations, we use, like for the basic approximation, the Van Leer fluxes which are in 1-D :
$f_1^+ = \frac{1}{4}\rho\, c\, \left(\frac{u}{c}+1\right)^2$, the flux $\mathcal{F}^+$ is given by :

$$\mathcal{F}^+ = \begin{cases} F & \text{if } u \geq c\ , \\ \begin{pmatrix} f_1^+ \\ \frac{f_1^+}{\gamma}((\gamma-1)u+2c) \end{pmatrix} & \text{if } -c < u < c\ , \\ 0 & \text{if } u \leq -c\ , \end{cases}$$

and $\mathcal{F}^-$ is obtained by : $\mathcal{F}^- = F - \mathcal{F}^+$

We note : $\tilde{\mathcal{F}}^+$ et $\tilde{\mathcal{F}}^-$ the Van Leer fluxes associated with the homenthalpic-flow approach, we have :

$$\tilde{\mathcal{F}}^+(\rho,\rho u) = \mathcal{F}^+(\rho,\rho u,E)$$

We can write :

$$\frac{\partial\tilde{\mathcal{F}}^+}{\partial X} = \frac{\partial\mathcal{F}^+}{\partial X} + \frac{\partial\mathcal{F}^+}{\partial E}\frac{\partial E}{\partial X} \quad \text{and} \quad \frac{\partial\tilde{\mathcal{F}}^-}{\partial X} = \frac{\partial\mathcal{F}^-}{\partial X} + \frac{\partial\mathcal{F}^-}{\partial E}\frac{\partial E}{\partial X}$$

The expressions of the energy E and the pressure p are :

$$E = \rho h_\infty - p \quad \text{et} \quad p = (\gamma-1)(E - \frac{1}{2}\rho u^2)$$

So :

$$E = \frac{\rho}{\gamma}(h_\infty + \frac{\gamma-1}{2}u^2)$$

Then, we write :

$$\frac{\partial E}{\partial \rho} = \frac{h_\infty - \frac{\gamma-1}{2}u^2}{\gamma}$$

$$\frac{\partial E}{\partial \rho u} = \frac{\gamma-1}{\gamma}u$$

We note $\tilde{A}^+$ the jacobian matrix of the flux $\tilde{\mathcal{F}}^+$ and $\tilde{A}^-$ the jacobian matrix of the flux $\tilde{\mathcal{F}}^-$. We now show that the eigenvalues of $\tilde{A}^+$ are positive and those of $\tilde{A}^-$ negative.

- Calculation of the eigenvalues of the jacobian matrix

Several cases are examined corresponding to a local supersonic or subsonic flow.
If $\boxed{u \geq c}$ (locally supersonic flow), we have :

$$\tilde{A}^+ = \begin{pmatrix} 0 & 1 \\ \dfrac{c^2-u^2}{\gamma} & \dfrac{\gamma+1}{\gamma}u \end{pmatrix} \qquad \text{et} \qquad \tilde{A}^- = 0$$

We note that the eigenvalues of $\tilde{A}^-$ are negative as desirable!
The eigenvalues of $\tilde{A}^+$ (in fact those of the exact jacobian matrix) verify :

$$\lambda^2 - \frac{\gamma+1}{\gamma}u\lambda + \frac{u^2-c^2}{\gamma} = 0$$

So, we have :

$$\lambda_1 = \frac{(\gamma+1)u - \sqrt{\Delta}}{2\gamma} \quad , \quad \lambda_2 = \frac{(\gamma+1)u + \sqrt{\Delta}}{2\gamma}$$

with :

$$\Delta = (\gamma-1)^2u^2 + 4\gamma c^2$$

Are λ_1 and λ_2 positive ?
We notice that λ_1 and λ_2 are positive if and only if $\dfrac{\gamma+1}{\gamma}u$ and $\dfrac{u^2-c^2}{\gamma}$ are positive, which is true because

$$u \geq c \geq 0.$$

So, the eigenvalues of $\tilde{A}$ are indeed positive.

Now, if $\boxed{-c < u < c}$ (locally subsonic flow), we have :

$$\tilde{A}^+ = \begin{pmatrix} A & B \\ \dfrac{A}{\gamma}C - uD & \dfrac{B}{\gamma}C + D \end{pmatrix}$$

and

$$\tilde{A}^- = \begin{pmatrix} -A & 1-B \\ \dfrac{c^2-u^2}{\gamma} - \dfrac{A}{\gamma}C + uD & \dfrac{\gamma+1}{\gamma}u - \dfrac{B}{\gamma}C - D \end{pmatrix}$$

where :

$$\begin{aligned} A &= \left(\frac{u}{c}+1\right)\left(1-\frac{u}{c}\right)\frac{c}{4}\left(1+\frac{\gamma-1}{2}\frac{u^2}{c^2}\right) \\ B &= \left(\frac{u}{c}+1\right)\left(\frac{1}{2}-(\gamma-1)\frac{u}{8c}+(\gamma-1)\frac{u^2}{8c^2}\right) \\ C &= (\gamma-1)u+2c \\ D &= \frac{\gamma-1}{\gamma}\left(1-\frac{u}{c}\right)\frac{c}{4}\left(\frac{u}{c}+1\right)^2 \end{aligned}$$

We notice that A and D are positive.

The two eigenvalues of $\tilde{A}^+$ verify :

$$\lambda^2-\alpha_1\lambda+\alpha_2=0$$

where :

$$\alpha_1 = A+D+\frac{B}{\gamma}C \quad \text{and} \quad \alpha_2 = D(A+uB)$$

So, we have :

$$\lambda_1=\frac{\alpha_1-\sqrt{\Delta}}{2} \quad , \quad \lambda_2=\frac{\alpha_2+\sqrt{\Delta}}{2}$$

with :

$$\Delta = {\alpha_1}^2-4\alpha_2$$

We note that λ_1 and λ_2 are positive if and only if α_1 et α_2 are also positive. But

$$\alpha_1\geq 0 \iff 4\gamma+4+2\left(1-\frac{u}{c}\right)+(\gamma-1)\frac{u^2}{c^2}\left(1-\frac{u}{c}\right)\geq 0$$

which is true because $u<c$.
α_2 is positive if and only if $A+uB$ is also positive. But

$$\begin{aligned} &A+uB\geq 0 \iff \\ &c\left(1-\frac{u}{c}\right)\left(1+\frac{\gamma-1}{2}\frac{u^2}{c^2}\right)+u\left(2-\frac{\gamma-1}{2}\frac{u}{c}+\frac{\gamma-1}{2}\frac{u^2}{c^2}\right)\geq 0 \iff \\ &c+u\geq 0 \end{aligned}$$

which is true because $u > -c$.
So, the eigenvalues of $\tilde{A}^+$ are indeed positive.
The two eigenvalues of $\tilde{A}^-$ verify :

$$\lambda^2 - \alpha_1 \lambda + \alpha_2 = 0$$

where :

$$\alpha_1 = -A - D - \frac{B}{\gamma} C + \frac{\gamma + 1}{\gamma} u$$

and

$$\alpha_2 = D(A + uB) - \frac{c^2 - u^2}{\gamma}(1 - B) - uD + 2(c - u)\frac{A}{\gamma}$$

So :

$$\lambda_1 = \frac{\alpha_1 - \sqrt{\Delta}}{2} \quad , \quad \lambda_2 = \frac{\alpha_2 + \sqrt{\Delta}}{2}$$

with :

$$\Delta = {\alpha_1}^2 - 4\alpha_2$$

We note that λ_1 and λ_2 are negative if and only if α_1 is negative and α_2 positive. But

$$\alpha_1 \leq 0 \iff$$
$$-\left(1 + \frac{u}{c}\right)\left(1 - \frac{u}{c}\right)\left(1 + \frac{\gamma - 1}{2}\frac{u^2}{c^2}\right) - 2(\gamma + 1)\left(1 - \frac{u}{c}\right) \leq 0$$

which is true because $-c < u < c$. Finally,

$$\alpha_2 \geq 0 \iff \left(\frac{u}{c} + 1\right)\left(1 - \frac{u}{c}\right)^2 \left(\frac{\gamma - 1}{16}\right)\left(1 + \frac{u^2}{c^2}\right) \geq 0$$

which is true because $u > -c$.
So, the eigenvalues of $\tilde{A}^-$ are indeed negative.

Let us consider now the last case $\boxed{u \leq -c}$ (supersonic reverse flow) :

$$\tilde{A}^- = \begin{pmatrix} 0 & 1 \\ \dfrac{c^2 - u^2}{\gamma} & \dfrac{\gamma + 1}{\gamma} u \end{pmatrix} \qquad \text{et} \qquad \tilde{A}^+ = 0$$

We note that the eigenvalues of $\tilde{A}^+$ are positive as expected!
The eigenvalues of $\tilde{A}^-$ (in fact those of the exact jacobian matrix) verify :

$$\lambda^2 - \frac{\gamma + 1}{\gamma} u\lambda + \frac{u^2 - c^2}{\gamma} = 0$$

Therefore :

$$\lambda_1 = \frac{(\gamma+1)u - \sqrt{\Delta}}{2\gamma} \quad , \quad \lambda_2 = \frac{(\gamma+1)u + \sqrt{\Delta}}{2\gamma}$$

with :

$$\Delta = (\gamma-1)^2 u^2 + 4\gamma c^2$$

Are λ_1 et λ_2 negative ?

We notice that λ_1 and λ_2 are positive if and only if $\frac{\gamma+1}{\gamma}u$ is negative and $\frac{u^2-c^2}{\gamma}$ positive. Which is true because

$$u \leq 0 \leq -c.$$

So, the eigenvalues of $\tilde{A}^-$ are indeed negative. □

In conclusion, the eigenvalues of the plus and minus parts of the jacobians of the considered flux-split forms are real and of the desirable signs, when the equivalent γ is assumed constant during the Euler substep (although not uniform through the domain). Hence, this trivial simplification of the flux-vector splitting applicable to homenthalpic flow is proved to realize on a stable discretization scheme.

In our approximation scheme, we usually use the Steger-Warming-like splitting for boundary conditions. For this reason, it is also necessary to examine how can the Steger-Warming splitting be restricted when the assumption of homenthalpic flow is made.

4.2.2 Jacobians of the Steger-Warming fluxes

For the Steger-Warming flux, the jacobian matrix is calculated in the same way :

$$\tilde{A} = \frac{\partial \tilde{\mathcal{F}}}{\partial X}$$

We have already calculated the eigenvalues of the exact jacobian matrix in the previous paragraph. These eigenvalues are :

$$\lambda_1 = \frac{(\gamma+1)u - \sqrt{\Delta}}{2\gamma} \quad , \quad \lambda_2 = \frac{(\gamma+1)u + \sqrt{\Delta}}{2\gamma}$$

with :

$$\Delta = (\gamma - 1)^2 u^2 + 4\gamma c^2$$

To calculate the Steger-Warming flux, one needs to know the eigenvectors of the jacobian matrix. We note r_1 and r_2 the two eigenvectors. We have :

$$r_1 = \begin{pmatrix} 1 \\ \lambda_1 \end{pmatrix} \quad \text{et} \quad r_2 = \begin{pmatrix} 1 \\ \lambda_2 \end{pmatrix}$$

The same calculation has been made in 2-D :
We note :
$\vec{n} = \begin{pmatrix} n_1 \\ n_2 \end{pmatrix}$ the vector normal to the interface through which we calculate the flux,
$u_n = u.n_1 + v.n_2 \quad \text{et} \quad v_n = v.n_1 - u.n_2$.
We note λ_1, λ_2 and λ_3 the eigenvalues and r_1, r_2 et r_3 the eigenvectors. We get :

$$\begin{aligned} \lambda_1 &= u_n \\ \lambda_2 &= \frac{(\gamma+1)u_n - \sqrt{\Delta}}{2\gamma} \\ \lambda_2 &= \frac{(\gamma+1)u_n + \sqrt{\Delta}}{2\gamma} \end{aligned}$$

where :

$$\Delta = (\gamma+1)^2 {u_n}^2 + 4\gamma(c^2 - u^2 - v^2)({n_1}^2 + {n_2}^2) + 4\gamma {v_n}^2$$

We note :

$$\begin{aligned} \alpha &= \frac{c^2}{(\gamma-1)v_n} \\ Z &= \frac{c^2 - u^2 - v^2}{\gamma} \\ N_i &= (\lambda_i - u_n)(Zn_1 + vv_n) - \frac{c^2}{\gamma} n_2 v_n + \left(1 - \frac{1}{\gamma}\right) u {v_n}^2 \\ M_i &= (\lambda_i - u_n)(Zn_2 - uv_n) + \frac{c^2}{\gamma} n_1 v_n + \left(1 - \frac{1}{\gamma}\right) v {v_n}^2 \\ D_i &= (\lambda_i - u_n)\left(\lambda_i - \left(1 + \frac{1}{\gamma}\right) u_n\right) + (1 - 1\gamma)\, {v_n}^2 \end{aligned}$$

We get :

$$r_1 = \begin{pmatrix} 1 \\ u - n_2\alpha \\ v + n_1\alpha \end{pmatrix} \quad , \quad r_i = \begin{pmatrix} 1 \\ N_i/D_i \\ M_i/D_i \end{pmatrix} \quad , \quad \text{for i=2,3}$$

In summary, we have proved that the trivial restriction of the Van Leer flux-vector splitting was a viable discretization approximation when the equivalent γ approach is used. And we have explicited the formulas of the Steger-Warming splitting in this context that are used in the boundary procedures.

These ingredients are implemented in a straightforward manner in the usual algorithm whose iterative properties are evaluated by numerical experiments in the next section.

4.3 SECOND ORDER FLUXES

For the spatial second order approximation, the jacobians matrices are the same than for the first order approximation, only the explicit fluxes change. We have calculated the homenthalpic second order fluxes from the homenthalpic first order fluxes in the same manner as we had calculated the standard second order fluxes.
We use the M.U.S.C.L. Van Leer approach in which the flow variables at nodes are replaced in the expression of the numerical fluxes by linear interpolates at the cell interface. The variables we use are : ρ, u, v (the primitive ones and not the conservative ones). The extrapolation of the variables are performed in the following way :

$$w_{ij} = w_i + \nabla w_i . \frac{\vec{ij}}{2}$$

where ∇w_i is the average gradient of the variable w at the node i. This average gradient can be calculated in several manners. In the "Quasi-TVD scheme based on the upwind triangle", we use an average between the prediction of a fully upwind scheme ($\nabla w_i = \nabla w_{T_{ij}}$ where T_{ij} is the "upwind" triangle) with that of a centered scheme by the Van Albada method :

$$\begin{aligned} \text{Ave(a,b)} &= \frac{(a^2+\epsilon)b + (b^2+\epsilon)a}{a^2+b^2+2\epsilon} && \text{if } ab > 0 \\ &= 0 && \text{otherwise} \end{aligned}$$

where ϵ is a small number to avoid 0 division.

5 NUMERICAL EXPERIMENTS

All our calculations have been made on a Convex C 210.
In all these calculations, we consider flows at 75 km of altitude and for a freestream Mach number of 25 (except in the paragraph 5.1 in which the freestream Mach number varies).These test-problems model strong chemical non equilibrium flows.

5.1 CALCULATIONS WITH THE BASIC ALGORITHM

We have calculated flows around a double ellipse geometry for various sizes (from 60 cm to 60 m). We note the CPU time of the implicit method and the number of iterations needed to obtain a reduction of the initial residual error by a factor of 10^{-4}.

Size	60 cm	6 m	60 m
no. of iterations	84	102	189
CPU time (sec)	327.58	391.18	720.36

Table 1 - Non-equilibrium flow; Efficiency of the standard algorithm

We note that despite these calculations simulate non-trivial flows (with regions of strong compression and rarefaction), the implicit scheme is very efficient and not so sensitive to variations in geometry size.

5.2 HOMENTHALPIC-FLOW CALCULATIONS

5.2.1 FIRST ORDER CALCULATIONS

In this paragraph, the ratio between the last and the first residual is 10^{-4}.
We have made calculations around a geometry of double ellipse for an inert gas and for a non-equilibrium gas. For both, we have noted the number of necessary iterations, the CFL used and the CPU time.
For the inert gas, we have the following results :

	Iterations	CFL	CPU time (sec)
standard	66	no limitation	150.00
homenthalpic	67	no limitation	117.81

Table 2 - Inert gas case; Efficiency of standard vs new algorithms

So, for the homenthalpic-flow method the CPU time needed to compute the solution is **22** % less than the CPU time needed for the standard method because 3 equations are solved instead of 4 with the same time step.
We have made the same experiment for a non-equilibrium gas, and we get the following results :

	Iterations	CFL	CPU time (sec)
standard	84	20	327.58
homenthalpic	62	no limitation	196.00

Table 3 - Non-equilibrium flow case (60 cm); Efficiency of standard vs new algorithms

For this case, the homenthalpic-flow approach was found more robust, the CFL could be increased and this resulted in a reduction of **40** % of the CPU time.
Another calculation has been made for a non-equilibrium flow for a size of the double ellipse of 6 m.

	Iterations	CFL	CPU time
standard	102	14	391.18
homenthalpic	86	25	272.46

Table 4 - Non-equilibrium flow case (6 m); Efficiency of standard vs new algorithms

We see that, even for a size of 6 m,the homenthalpic-flow approach increases the robustness of the scheme, the CFL could be increased and this resulted in a reduction of **30** % of the CPU time. Hence, this method is more efficient than the basic one.
Another influence of this method is the changes we observe on the flow calculated. For the solution calculated for an inert gas (fig. 1), we see that the temperarure at the stagnation point decreases from 28566 K to 25755 K (the known exact value is 25869 K), so we obtain a value very close to the correct one.
Concerning the solution of the flow around a double ellipse of 60 cm (fig.2), we see that the temperature in the shock increases (from 16909 K to 17049 K), that is the peak is somewhat better represented; farther, the temperature at the stagnation point decreases (from 11249 K to 10719 K) which is far from, but somewhat closer, to the expected value. For the flow around the double ellipse of 6 m (fig. 3), we also observe that the temperature in the shock increases (from 13647 K to 14216 K) and the temperature at the stagnation point decreases (from 8548 K to 8252 K).
In conclusion, in hypersonic flow applications in which the level of enthalpy is high by nature, it is found unsurprisingly, that solving the energy equation exactly results in improvements of accuracy.

INERT GAS SOLUTION

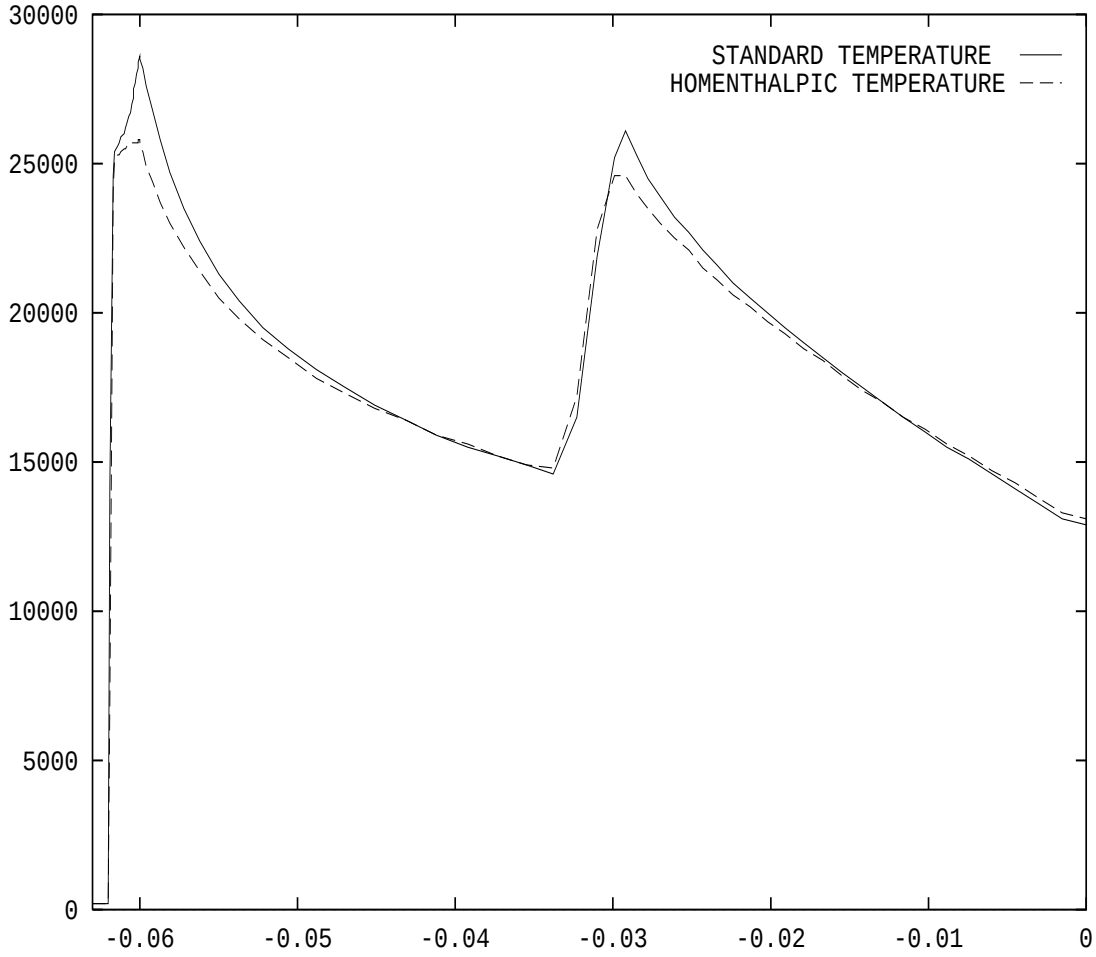

fig. 1

NON-EQUILIBRIUM GAS - 60 CM

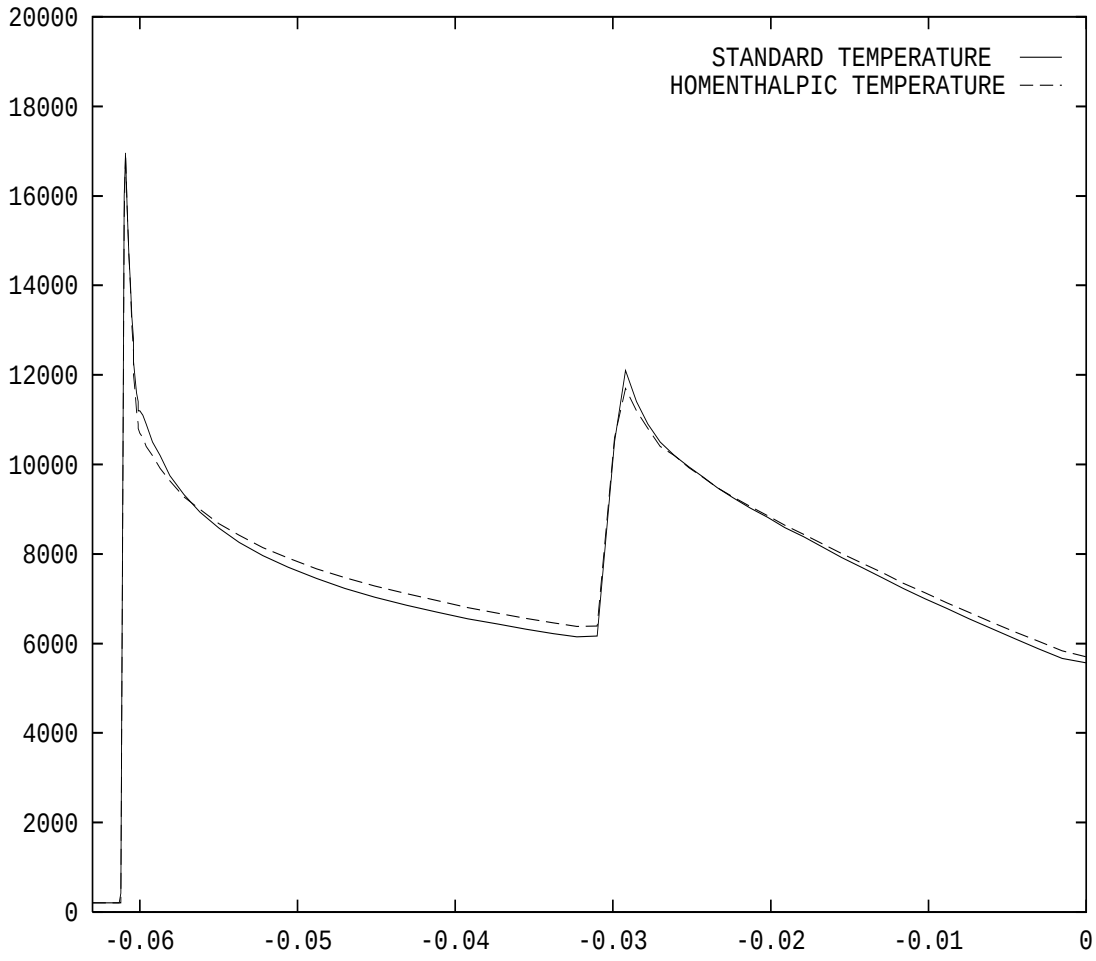

fig. 2

NON-EQUILIBRIUM GAS - 6 M

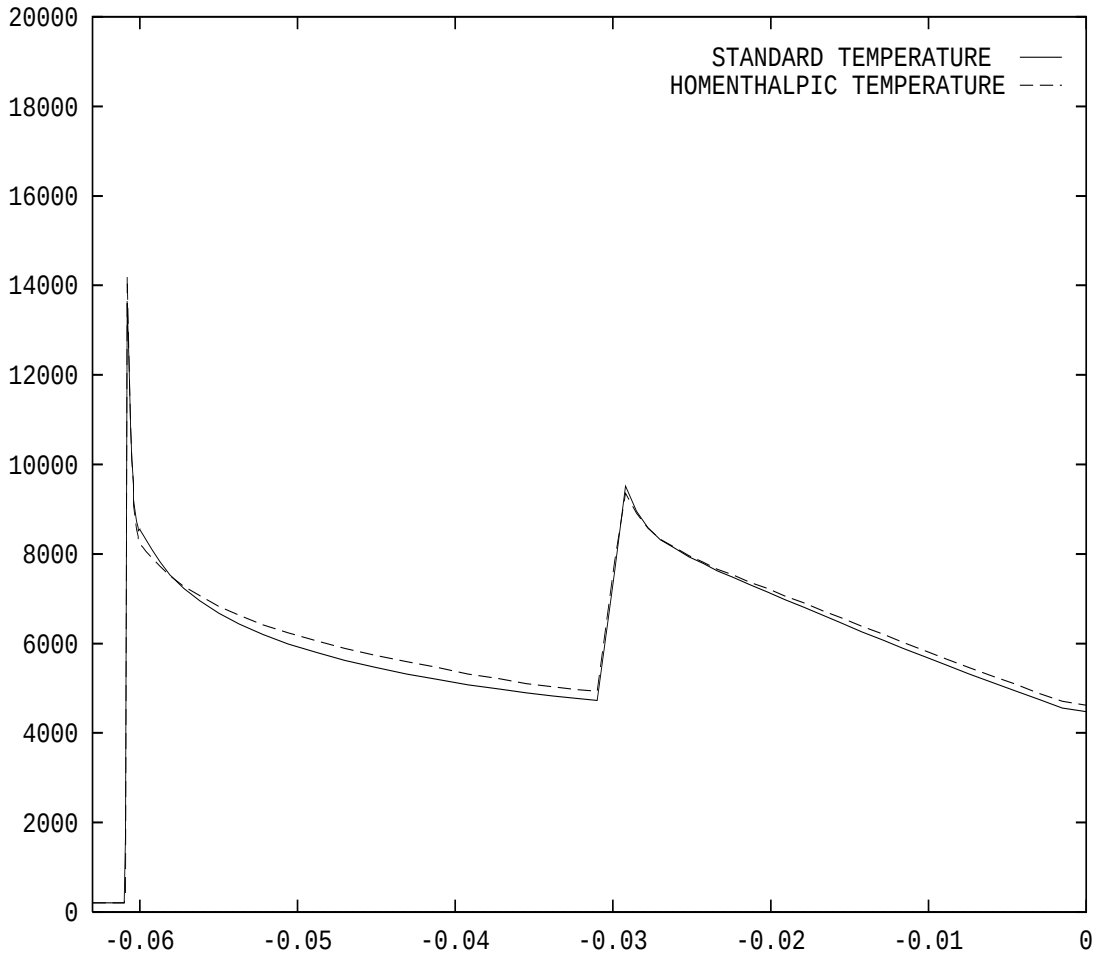

fig. 3

5.2.2 SECOND ORDER CALCULATIONS

We have made second order calculations on the previous mesh of double ellipse (2025 points) to compare with the first order solution. And then, we have computed the solution on a twice refined mesh of 14388 points to have a more accurate solution.
We see (fig. 4) that the homenthalpic second order solution on the 2025 points mesh increases significantly the temperature in the shock (from 17049 K to 18332 K), decreases the temperature at the stagnation point (from 10719 K to 9943 K) and on the body, which is suitable.
We present on the figure 5 the twice refined mesh of 14388 points. On the figure 6 we can see the temperature-lines of the standard second order method and on the figure 7 those of the homenthalpic second order one. The temperature-lines are somewhat different for the two methods especially after the canopy shock perhaps because the homenthalpic method is less diffusive. We see that the shock is very well captured for the two algorithms but a little better for the homenthalpic method (18949 K for the homenthalpic method instead of 18812 K for the standard one), the value at the stagnation point is about the same (8406 K).
The homenthalpic second order scheme is of course more accurate than the homenthalpic first order one, but also a little more accurate than the standard second order scheme.

DOUBLE ELLIPSE - 2025 POINTS
FIRST ORDER - SECOND ORDER COMPARISON

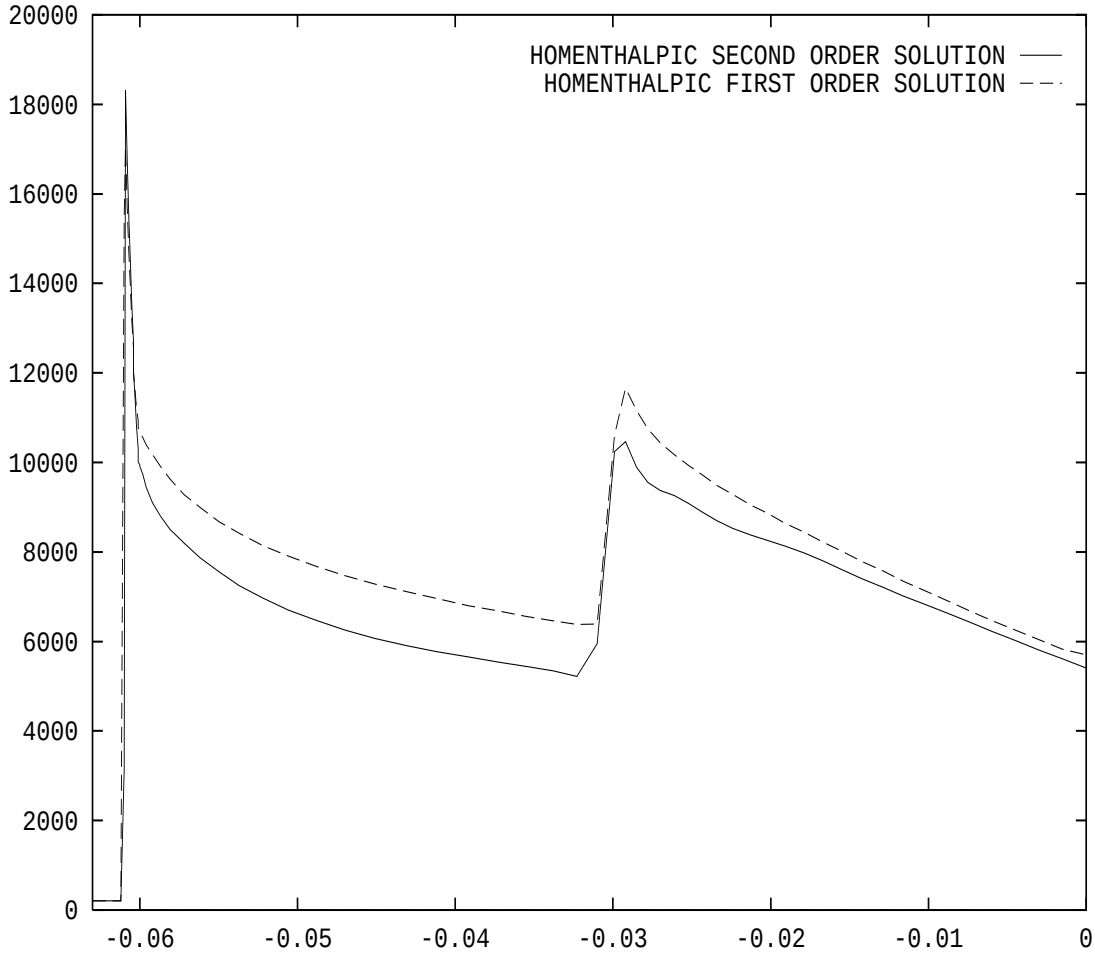

fig. 4

DOUBLE ELLIPSE 14338 POINTS

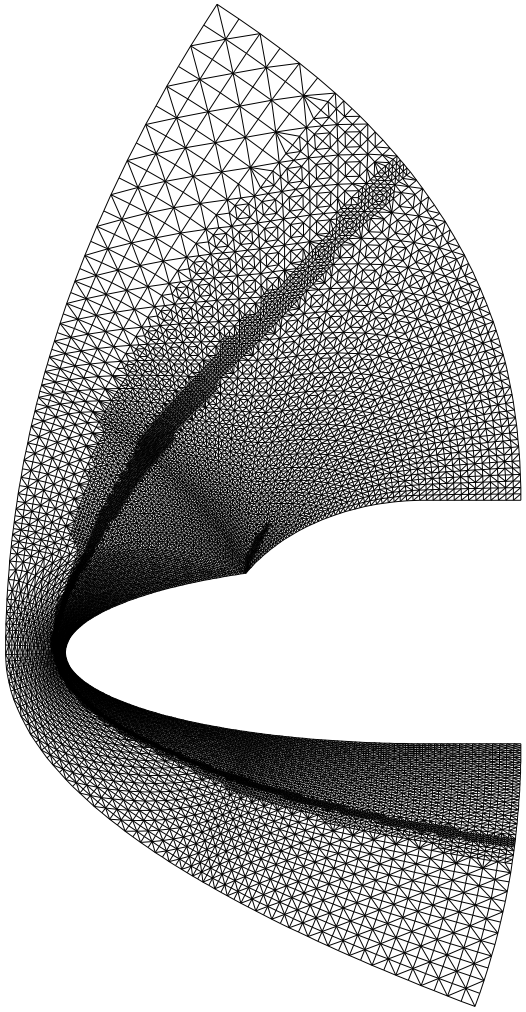

fig. 5

STANDARD SECOND ORDER - HOMENTHALPIC SECOND ORDER

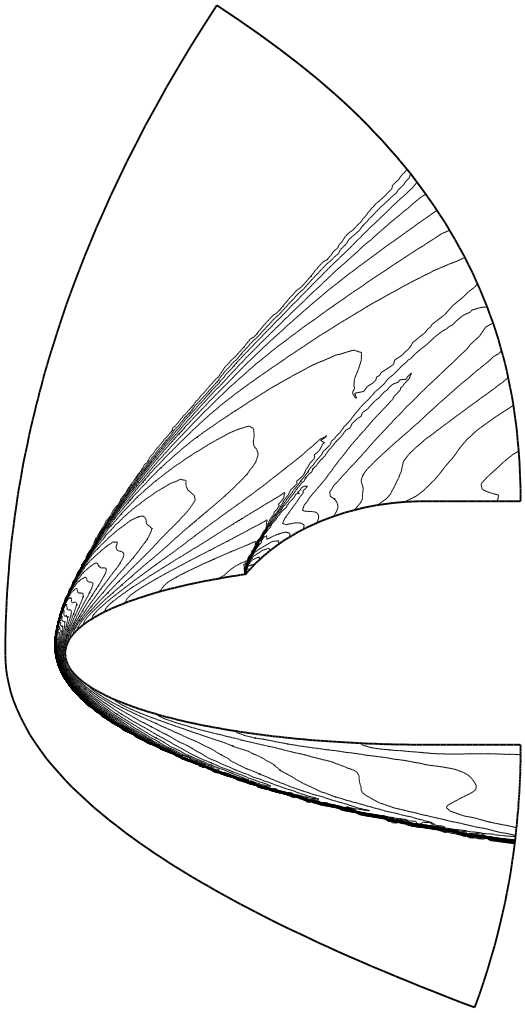

fig. 6

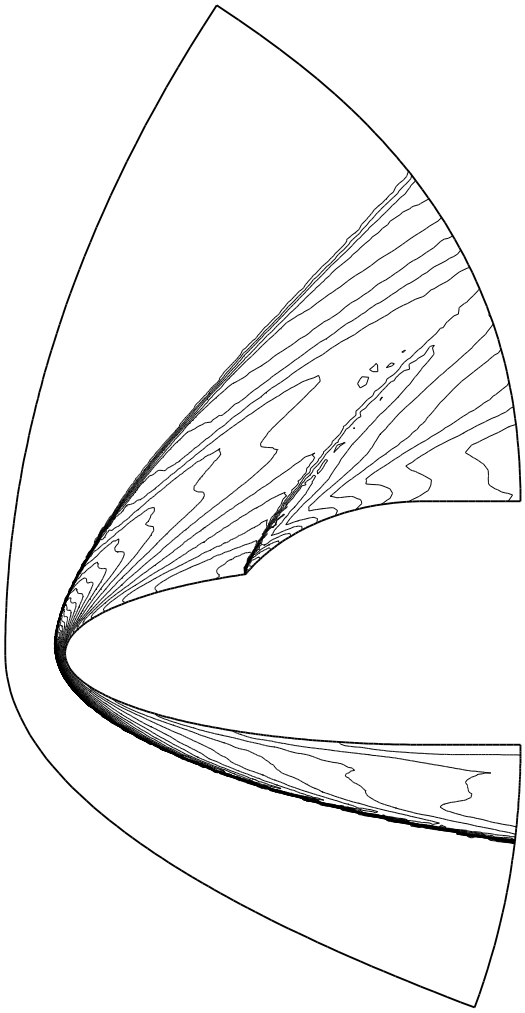

fig. 7

6 CONCLUSIONS

A steady inviscid supersonic flow is homenthalpic when it is subject to uniform inflow boundary conditions. This study is situated in a context where this assumption is verified.

For this case, the jacobian matrices of the Van Leer and the Steger-Warming flux-vector splittings, their eigenvalues and their eigenvectors have been formely calculated. We have shown that the Van Leer flux vector splitting is proper in this restriction (the eigenvalues of A^+ are positive and those of A^- are negative).

The homenthalpic-flow algorithm is found more efficient for external inviscid non-equilibrium flows. The robustness of the basic method is increased (it was already efficient and not too sensitive in variations in size). Its effects on the solutions are the increase of the temperature in the shock and the decrease of the temperature at the stagnation point; in other words, the accuracy is somewhat improved.

We have also computed the second order homenthalpic scheme, which is, of course, more accurate than the first order homenthalpic and second order standard ones.

Hence, although limited to homenthalpic flow, the new method is rather attractive from both efficiency and accuracy standpoints.

References

[1] Y. B. ZEL'DOVICH, Y. P. RAIZER, "Physic of Shock Waves and High Temperature Hydrodynamic Phenomena", *Academic Press.*

[2] C. PARK, "On The Convergence of Chemically Reacting Flows", *AIAA Paper 85-0247, AIAA 23rd Aerospace Sciences Meeting, Reno/Nevada, January 14-17, 1985.*

[3] B. Van LEER, "Towards the Ultimate Conservative Difference Scheme III", *J. Comput. Phys. 23,263-275, 1977.*

[4] J-A. DESIDERI, N. GLINSKY, E. HETTENA, "Hypersonic Reactive Flows Computation", *Computers and Fluids Journal Vol.18, No.2, pp.151-182, 1990.*

[5] M. C. CICCOLI, L. FEZOUI, J-A. DESIDERI, "Méthodes Numériques Efficaces pour les Ecoulements Hypersoniques Non Visqueux Hors Equilibre Chimique", *La Recherche Aerospatiale, 1992-1, 1992.*

[6] B. LARROUTUROU, L. FEZOUI, "On the Equation of Multi-Component Perfect or Real Gas Inviscid Flow", *Non Linear Hyperbolic Problems, Carasso, Charrier, Hanouzt and Joly Eds, Lecture Notes on Mathematics, Springer-Verlag, Heidelberg, 1989.*

[7] N. BOTTA, M.C. CICCOLI, J.A. DESIDERI, L. FEZOUI, N. GLINSKY, E. HETTENA, C. OLIVIER, " Reactive Flow Computations by Upwind Finite Elements ", *Proc. of INRIA-GAMNI/SMAI Workshop on Hypersonic Flows for Reentry Problems, January 22-25, 1990, Antibes, to appear in Springer-Verlag.*